Nuclear magnetic shielding and chirality. III. The single electron on a helix model

Devin N. Sears and Cynthia J. Jameson
Department of Chemistry M/C-111, University of Illinois at Chicago, Chicago, Illinois 60607-7061

Robert A. Harris
Department of Chemistry, University of California at Berkeley, Berkeley, California 94720

(Received 24 February 2003; accepted 5 May 2003)

In this third paper of the triptych we use the Tinoco–Woody model of an electron on a helix as our chiral system [I. Tinoco, Jr. and R. W. Woody, J. Chem. Phys. **40**, 160 (1964)]. Diastereomerism is achieved by varying the pitch of the helix. The full nuclear magnetic shielding tensor of a naked spin is determined with various subtleties explicated. The results are compared to the Ne helix diastereomers. © *2003 American Institute of Physics.* [DOI: 10.1063/1.1586700]

I. INTRODUCTION

We examine the nuclear magnetic shielding tensor of a naked spin interacting with an electron constrained to move on a helix: The Tinoco–Woody model.[1] The electron on a helix is the simplest model of a particle in a chiral potential whose properties may be determined nonperturbatively in the chiral potential. It is also the simplest model that manifests diastereomerism.

The earliest model of an electron in a chiral potential is that of Condon and Eyring.[2] The electron is subject to an asymmetric harmonic oscillator potential,

$$V_0(\mathbf{r}) = \sum_{i,j} a_{ij} x_i x_j , \tag{1}$$

a potential which is even under parity. The states and eigenvalues may be determined exactly. The oscillator is then perturbed by the anharmonic potential,

$$V_1(\mathbf{r}) = \lambda xyz, \tag{2}$$

which, itself, is odd under parity. The total potential is chiral. Hence, to first order in V_1 and exactly in V_0, chirality emerges.

In 1964 Tinoco and Woody exactly solved for the states and eigenvalues of an electron constrained to live on a space curve helix: the ''free'' electron on a helix model.[1] They calculated the rotational strengths and optical activity of this system. They showed the optical activity of helical copper wires were in agreement with the model in the appropriate frequency range.[1,3] Balazs *et al.*[4] showed in detail how to obtain the states, eigenvalues, and optical properties of an electron constrained to any space curve, including helices. Maki and Persoons[5] used the same model, albeit classically, to model the second-order nonlinear response of electrons in chiral potentials. Very recently, Rikken *et al.* determined the magnetochiral anisotropy of an electron on a helix.[6] Unlike the other uses of the model, which are finite frequency responses, the shielding is a static response.

II. MODEL

A. Electron constrained to a helix

Parenthetically we point out that the use of ''free electron'' is a misnomer. The electron is constrained on the helix. The constraints may be realized through subjecting the particle to a three-dimensional potential, and limiting the behavior in directions normal to the space curve to the ground state in those directions, or else by having the constraints to begin with. The latter gives operators that are not necessarily Hermitian. Demanding Hermiticity yields additional terms in various matrix elements. This point will be made clearer when we look at the nuclear magnetic shielding tensor.

We now briefly discuss the model. In particular we define diastereomerism in the context of the model. In the main we follow the notation of Tinoco and Woody.[1] The axis of the helix is taken to be parallel to the z axis. We shall place the naked spin at the origin since this simplifies the calculation. Although the number of turns below the XY plane need not equal the amount above the plane, we shall consider the limiting cases: (a) the spin is in the middle of the helix, and, (b) the spin is at the beginning of the helix.

A space helix may be described in terms of three parameters. If the helix is wrapped around a cylinder parallel to the z axis, then the position vector for the helix may be written as

$$\mathbf{r}(\theta) = \mathbf{i}a\cos\theta + \mathbf{j}a\sin\theta + \mathbf{k}b\theta \tag{3}$$

with

$$-k\pi \leqslant \theta \leqslant k\pi \tag{4}$$

for case (a), and

$$0 \leqslant \theta \leqslant k2\pi \tag{5}$$

for case (b). The radius of the helix is a, $2\pi b$ is the pitch, and k is the number of turns. The handedness of the helix is given by $b(>0)$. $+b$ is a right-handed helix (R) and $-b$ is a left handed helix (L).

We express diastereomerism by adding or subtracting an additional pitch d (>0). We shall subsume all combinations in a pitch, $2\pi\beta$. Thus we define diastereomer combinations as

$$Rr: \quad \beta=(b+d), \tag{6a}$$

$$Rl: \quad \beta=(b-d), \tag{6b}$$

$$Lr: \quad \beta=(-b+d), \tag{6c}$$

$$Ll: \quad \beta=(-b-d). \tag{6d}$$

Because the axis of the helix is in the Z direction, the operation of reflection in the XY plane and subsequent rotation by π about an axis in the XY plane is equivalent to $\beta\rightarrow-\beta$. We shall further clarify this when we consider the angular momentum operators.

By conservation of parity, any scalar property (S) must obey

$$\mathrm{S}(Rr)=\mathrm{S}(Ll) \text{ and } \mathrm{S}(Rl)=\mathrm{S}(Lr).$$

Any splitting must be

$$\mathrm{S}(Rr)-\mathrm{S}(Rl) \text{ or } \mathrm{S}(Ll)-\mathrm{S}(Lr).$$

Concomitantly, any pseudoscalar property (PS) must have

$$\mathrm{PS}(Rr)=-\mathrm{PS}(Ll) \text{ and } \mathrm{PS}(Rl)=-\mathrm{PS}(Lr).$$

In terms of β it is clear that all scalar properties will be even functions of β and all pseudoscalar properties will be odd functions of β explicitly.

The details of the model, the construction of various operators, the eigenstates and eigenvalues of the electron on the helix may be found in the papers of Tinoco and Woody[1] and Tobias *et al.*[4] Here we just quote the results necessary to exhibit diastereomerism within the model. First we consider the eigenvalues. They are, as usual,

$$E_n=\hbar^2n^2/8mk^2(a^2+\beta^2), \quad n=1,\ 2,\ldots\ . \tag{7}$$

Hence

$$E_n(Rr)=E_n(Ll)\propto\{1/[a^2+(b+d)^2]\} \tag{8}$$

and

$$E_n(Rl)=E_n(Lr)\propto\{1/[a^2+(b-d)^2]\}. \tag{9}$$

Ll and *Rr* represent stretching the helix. *Rl* and *Lr* represent compression. For $b\gg d$, weak diastereomers, we have

$$E_n(Rr)-E_n(Ll)\propto-4bd/(a^2+b^2). \tag{10}$$

In this simple model it is always the case that

$$E_n(Rr)<E_n(Rl). \tag{11}$$

We now construct the shielding tensor for a naked spin interacting with an electron on a helix. For convenience we shall present the method of calculation where the spin is in the middle of the helix. A textbook extension of Tinoco and Woody's calculation yields as eigenfunctions

$$\Psi_m(\theta)=(k\pi)^{-1/2}\cos(m\theta/2k), \quad m=1,\ 3,\ 5,\ldots, \tag{12a}$$

$$\Psi_m(\theta)=(k\pi)^{-1/2}\sin(m\theta/2k), \quad m=2,\ 4,\ 6,\ldots\ . \tag{12b}$$

It is important to realize that the eigenstates do not "know" whether the helix is *L* or *R*, or *Ll*, or *Lr*. All aspects of chirality appear in the operators.

B. Shielding tensor of a naked spin interacting with the electron constrained to a helix

A shielding tensor element of a single electron interacting with a naked spin at the origin is given by

$$\sigma_{ij}=(e^2/mc^2)\langle g|(\mathbf{1}\rho^2-\rho_i\rho_j)/\rho^3|g\rangle-[\hbar^2e^2/(2mc^2)^2]\times\sum_{v'}\{\langle g|L_i|v\rangle\langle v|L_j/\rho^3|g\rangle+\langle g|L_j/\rho^3|v\rangle\langle v|L_i|g\rangle\}/(E_v-E_g). \tag{13}$$

Here $|g\rangle$ labels the ground state, v the excited state; ρ is the distance from the origin, and L_i is the dimensionless angular momentum operator of the electron. As written σ_{ij} is a reducible second rank tensor.

We now come to a fundamental subtlety that does not occur when the particle is in a nonsingular three-dimensional potential. When the particle is constrained to a space curve, the usual commutation relations between position and momenta do not hold. Hence the angular momentum operators are not Hermitian. In addition, the angular momentum does not commute with the scalar distance. This situation may be ameliorated in two ways: first by constructing Hermitian operators, second by constructing eigenstates in three dimensions and taking the appropriate limits. For a particle constrained to move on a circle the second method is what is normally done. For a particle constrained to live on a helix this goal can be approximately accomplished. In either case, there are extra terms in the matrix elements that appear in physical responses such as the optical activity, and we shall see, the shielding tensor. We shall follow the second method, though the first is more satisfying. In the Appendices we give the Hermitian version of the angular momentum operators and (L_i/ρ^3) for a particle on a helix.

III. RESULTS

We considered two cases: Case (a), the naked spin located at the center of the helix, helix limits are $-k\pi$ to $+k\pi$, and Case (b), the naked spin located at the end of the helix, helix limits are 0 to $+k2\pi$. The eigenfunctions for case (a) are given in Eq. (12) while those for case (b) are given by Tinoco and Woody.[1] The parameters are chosen to be the same as those used for the Ne_8 helix in Paper II,[7] so that comparison may be made with this system: $a=$radius $=3.260$ Å, $k=(1+1/7)=1.142\,857$, equivalent to that used for the Ne_8 helix (electrons of Ne assumed to extend to half the distance between Ne atoms in the helix). $|b|=0.557\,042$ Å rad^{-1}, to have the same pitch as was used for the Ne_8 helix and $|d|=0.055\,704\,2$ Å rad^{-1}, 10% of $|b|$. Numerical precision was chosen to be the maximum permitted by Mathematica,[8] for all numerical steps. We checked for convergence of the sum over n. The paramagnetic sum converged fast. Going up to $n=50$ does not increase the accuracy sufficiently to warrant the effort. Unlike all other mod-

TABLE I. Shielding tensor components for a naked spin at the center of a helix [case (a)].

Term	*R* $\beta=+b$	*L* $\beta=-b$	*Rr* $\beta=+b+d$	*Ll* $\beta=-b-d$	*Rl* $\beta=+b-d$	*Lr* $\beta=-b+d$
$\sigma_{XX}^{\text{diam}}$	2.213 75	2.213 75	2.211 25	2.211 25	2.215 58	2.215 58
$\sigma_{YY}^{\text{diam}}$	2.191 44	2.191 44	2.206 79	2.206 79	2.176 81	2.176 81
$\sigma_{ZZ}^{\text{diam}}$	4.042 84	4.042 84	3.992 51	3.992 51	4.090 55	4.090 55
$\sigma_{\text{iso}}^{\text{diam}}$	2.816 01	2.816 01	2.803 51	2.803 51	2.827 64	2.827 64
$\sigma_{XX}^{\text{param}}$	−0.107 497	−0.107 497	−0.124 227	−0.124 227	−0.090 889 4	−0.090 889 4
$\sigma_{YY}^{\text{param}}$	−0.183 184	−0.183 184	−0.217 469	−0.217 469	−0.151 01	−0.151 01
$\sigma_{ZZ}^{\text{param}}$	−3.450 98	−3.450 98	−3.309 15	−3.309 15	−3.589 48	−3.589 48
$\sigma_{\text{iso}}^{\text{param}}$	−1.247 22	−1.247 22	−1.216 95	−1.216 95	−1.277 13	−1.277 13
σ_{iso}	1.568 79	1.568 79	1.586 57	1.586 57	1.550 52	1.550 52
$\sigma_{XY}^{\text{diam}}$	0.	0.	0.	0.	0.	0.
$\sigma_{YX}^{\text{diam}}$	0.	0.	0.	0.	0.	0.
$\sigma_{XZ}^{\text{diam}}$	0.	0.	0.	0.	0.	0.
$\sigma_{ZX}^{\text{diam}}$	0.	0.	0.	0.	0.	0.
$\sigma_{YZ}^{\text{diam}}$	−0.542 343	0.542 343	−0.584 021	0.584 021	−0.497 858	0.497 858
$\sigma_{ZY}^{\text{diam}}$	−0.542 343	0.542 343	−0.584 021	0.584 021	−0.497 858	0.497 858
$\sigma_{XY}^{\text{param}}$	0.	0.	0.	0.	0.	0.
$\sigma_{YX}^{\text{param}}$	0.	0.	0.	0.	0.	0.
$\sigma_{XZ}^{\text{param}}$	0.	0.	0.	0.	0.	0.
$\sigma_{ZX}^{\text{param}}$	0.	0.	0.	0.	0.	0.
$\sigma_{YZ}^{\text{param}}$	0.719 774	−0.719 774	0.759 66	−0.759 66	0.673 377	−0.673 377
$\sigma_{ZY}^{\text{param}}$	0.820 592	−0.820 592	0.886 768	−0.886 768	−0.750 708	−0.750 708
σ_{XX}	2.106 25	2.106 25	2.087 02	2.087 02	2.124 69	2.124 69
σ_{YY}	2.008 25	2.008 25	1.989 32	1.989 32	2.025 8	2.025 8
σ_{ZZ}	0.591 864	0.591 864	0.683 361	0.683 361	0.501 07	0.501 07
σ_{XY}	0.	0.	0.	0.	0.	0.
σ_{YX}	0.	0.	0.	0.	0.	0.
σ_{XZ}	0.	0.	0.	0.	0.	0.
σ_{ZX}	0.	0.	0.	0.	0.	0.
σ_{YZ}	0.177 431	−0.177 431	0.175 639	−0.175 639	0.175 52	−0.175 52
σ_{ZY}	0.278 249	−0.278 249	0.302 747	−0.302 747	0.252 85	−0.252 85
$\frac{1}{2}[\sigma_{XY}+\sigma_{YX}]$	0.	0.	0.	0.	0.	0.
$\frac{1}{2}[\sigma_{XZ}+\sigma_{ZX}]$	0.	0.	0.	0.	0.	0.
$\frac{1}{2}[\sigma_{YZ}+\sigma_{ZY}]$	0.227 84	−0.227 84	0.239 193	−0.239 193	0.214 185	−0.214 185
$\frac{1}{2}[\sigma_{XY}-\sigma_{YX}]$	0.	0.	0.	0.	0.	0.
$\frac{1}{2}[\sigma_{XZ}-\sigma_{ZX}]$	0.	0.	0.	0.	0.	0.
$\frac{1}{2}[\sigma_{YZ}-\sigma_{ZY}]$	−0.050 409	0.050 409	−0.063 554 1	0.063 554 1	−0.038 665 2	0.038 665 2

els, and systems, the paramagnetic shielding tensor may be exactly determined. As a practical decision, we evaluated all results reported here using $n=2$ to 30.

The calculated individual components for case (a) are shown in Table I and those for case (b) are shown in Table II. Comparisons of compressed (*Lr* and *Rl*) and stretched (*Ll* and *Rr*) helices with the reference helix (*L* and *R*) are interesting. The important conclusions are unchanged from the $n@\text{Ne}_8$ (Ref. 7) or the $\text{Xe}@\text{Ne}_8$ calculations.[9] It is important to note that the symmetry at the site of the naked spin, rather than the molecular symmetry, governs the number of nonvanishing distinct shielding tensor components.

(i) The principal components of the symmetric part of the shielding tensor in corresponding chiral models are the same for *R* as for *L*, the same for *Rr* as for *Ll*, the same for *Rl* as for *Lr*. This is exhibited in Table I for case (a), as well as in Table II for case (b). The corresponding diagonal elements of the symmetric part of the tensors are identical and the magnitudes of the corresponding off-diagonal elements match.

(ii) Since the helical axis is chosen along the *Z* direction in the laboratory frame, the signs of the off-diagonal elements (hence the antisymmetric tensor elements also) are reversed for the components involving *Z*, when the handedness of the helix is changed from *R* to *L* in all cases. The off-diagonal elements involving only *X* and *Y* do not change sign (the antisymmetric tensor elements also). This corresponds to a rotation of the principal axes in going from *R* to *L*.

(iii) The symmetry of the site of the naked spin in the case (a) system is such that there is a C_2 axis (coordinates are defined such that this symmetry axis is the laboratory $-X$ axis) perpendicular to the helical axis, in which case σ_{XZ} and σ_{XY}, σ_{ZX}, and σ_{YX} are all zero by symmetry for both the diamagnetic and the paramagnetic components. Thus one principal axis of the symmetric part of the shielding tensor lies along the laboratory *X* axis and the only off-diagonal symmetric component is $\frac{1}{2}[\sigma_{YZ}+\sigma_{ZY}]$. This symmetry is not present in the case (b) system so there are off-diagonal components in both the diamagnetic and the paramagnetic parts for case (b).

TABLE II. Shielding tensor components for a naked spin at the end of a helix [case (b)].

Term	R $\beta=+b$	L $\beta=-b$	Rr $\beta=+b+d$	Ll $\beta=-b-d$	Rl $\beta=+b-d$	Lr $\beta=-b+d$
$\sigma_{XX}^{\text{diam}}$	2.325 48	2.325 48	2.324 59	2.324 59	2.321 98	2.321 98
$\sigma_{YY}^{\text{diam}}$	2.300 69	2.300 69	2.298 13	2.298 13	2.297 03	2.297 03
$\sigma_{ZZ}^{\text{diam}}$	2.711 56	2.711 56	2.523 73	2.523 73	2.909 63	2.909 63
$\sigma_{\text{iso}}^{\text{diam}}$	2.445 91	2.445 91	2.382 15	2.382 15	2.509 55	2.509 55
$\sigma_{XX}^{\text{param}}$	−0.495 095	−0.495 095	−0.544 086	−0.544 086	−0.440 986	−0.440 986
$\sigma_{YY}^{\text{param}}$	−0.511 945	−0.511 945	−0.555 678	−0.555 678	−0.461 152	−0.461 152
$\sigma_{ZZ}^{\text{param}}$	−2.634 54	−2.634 54	−2.437 52	−2.437 52	−2.842 3	−2.842 3
$\sigma_{\text{iso}}^{\text{param}}$	−1.213 86	−1.213 86	−1.179 09	−1.179 09	−1.248 15	−1.248 15
σ_{iso}	1.232 05	1.232 05	1.203 05	1.203 05	1.261 4	1.261 4
$\sigma_{XY}^{\text{diam}}$	0.013 341 7	0.013 341 7	0.013 866	0.013 866	0.012 773 5	0.012 773 5
$\sigma_{YX}^{\text{diam}}$	0.013 341 7	0.013 341 7	0.013 866	0.013 866	0.012 773 5	0.012 773 5
$\sigma_{XZ}^{\text{diam}}$	0.576 092	−0.576 092	0.600 589	−0.600 589	0.543 762	−0.543 762
$\sigma_{ZX}^{\text{diam}}$	0.576 092	−0.576 092	0.600 589	−0.600 589	0.543 762	−0.543 762
$\sigma_{YZ}^{\text{diam}}$	0.379 758	−0.379 758	0.352 074	−0.352 074	0.401 632	−0.401 632
$\sigma_{ZY}^{\text{diam}}$	0.379 758	−0.379 758	0.352 074	−0.352 074	0.401 632	−0.401 632
$\sigma_{XY}^{\text{param}}$	−0.005 714 14	−0.005 714 14	−0.008 427 67	−0.008 427 67	−0.002 854 53	−0.002 854 53
$\sigma_{YX}^{\text{param}}$	−0.005 713 93	−0.005 713 93	−0.008 427 38	−0.008 427 38	−0.002 854 38	−0.002 854 38
$\sigma_{XZ}^{\text{param}}$	−0.554 872	0.554 872	−0.586 356	0.586 356	−0.515 84	0.515 84
$\sigma_{ZX}^{\text{param}}$	−0.554 874	0.554 874	−0.586 358	0.586 358	−0.515 842	0.515 842
$\sigma_{YZ}^{\text{param}}$	−0.560 637	0.560 637	−0.536 994	0.536 994	−0.576 009	0.576 009
$\sigma_{ZY}^{\text{param}}$	−0.560 639	0.560 639	−0.536 997	0.536 997	−0.576 011	0.576 011
σ_{XX}	1.830 39	1.830 39	1.780 5	1.780 5	1.880 99	1.880 99
σ_{YY}	1.788 75	1.788 75	1.742 45	1.742 45	1.835 88	1.835 88
σ_{ZZ}	0.077 019 4	0.077 019 4	0.086 209	0.086 209	0.067 321 7	0.067 321 7
σ_{XY}	0.007 627 54	0.007 627 54	0.005 438 32	0.005 438 32	0.009 919 01	0.009 919 01
σ_{YX}	0.007 627 75	0.007 627 75	0.005 438 61	0.005 438 61	0.009 919 16	0.009 919 16
σ_{XZ}	0.021 219 7	−0.021 219 7	0.014 233 1	−0.014 233 1	0.027 922	−0.027 922
σ_{ZX}	0.021 217 9	−0.021 217 9	0.014 231	−0.014 231	0.027 920 4	−0.027 920 4
σ_{YZ}	−0.180 878	0.180 878	−0.184 92	0.184 92	−0.174 377	0.174 377
σ_{ZY}	−0.180 881	0.180 881	−0.184 923	0.184 923	−0.174 379	0.174 379
$\frac{1}{2}[\sigma_{XY}+\sigma_{YX}]$	0.007 627 64	0.007 627 64	0.005 438 46	0.005 438 46	0.009 919 08	0.009 919 08
$\frac{1}{2}[\sigma_{XZ}+\sigma_{ZX}]$	0.021 218 8	−0.021 218 8	0.014 232 1	−0.014 232 1	0.027 921 2	−0.027 921 2
$\frac{1}{2}[\sigma_{YZ}+\sigma_{ZY}]$	−0.180 879	0.180 879	−0.184 922	0.184 922	−0.174 378	0.174 378
$\frac{1}{2}[\sigma_{XY}-\sigma_{YX}]$	$-1.076\,16\times10^{-7}$	$-1.076\,16\times10^{-7}$	$-1.463\,97\times10^{-7}$	$-1.463\,97\times10^{-7}$	$-7.476\,2\times10^{-8}$	$-7.476\,2\times10^{-8}$
$\frac{1}{2}[\sigma_{XZ}-\sigma_{ZX}]$	$9.152\,25\times10^{-7}$	$-9.152\,25\times10^{-7}$	$1.061\,28\times10^{-6}$	$-1.061\,28\times10^{-6}$	$7.678\,25\times10^{-7}$	$-7.678\,25\times10^{-7}$
$\frac{1}{2}[\sigma_{YZ}-\sigma_{ZY}]$	$1.360\,45\times10^{-6}$	$-1.360\,45\times10^{-6}$	$1.565\,62\times10^{-6}$	$-1.565\,62\times10^{-6}$	$1.151\,72\times10^{-6}$	$-1.151\,72\times10^{-6}$

(iv) The shielding tensor has a nonvanishing antisymmetric part in a chiral environment. In case (a), as described above, the only off-diagonal paramagnetic components are σ_{YZ} and σ_{ZY}, thus the only antisymmetric component in case (a) is
$\frac{1}{2}[\sigma_{YZ}-\sigma_{ZY}]=-0.050\,409$ ppm for R and
$+0.050\,409$ ppm for L,
as can be seen in Table I. In principle, three different antisymmetric components do not vanish in case (b). Unfortunately, these antisymmetric components are all small, as seen in Table II. The naked spin is only close to the electron at the one end of the helix where the boundary conditions makes all the wave functions vanish.

(i) There is a chiral shift. That is, there is a shielding difference between (Rr, Ll) and (Rl, Lr). For n@helix, the diamagnetic parts alone give
$\sigma_{\text{iso}}^{\text{diam}}(Lr,\ Rl)>\sigma_{\text{iso}}^{\text{diam}}(Ll,\ Rr)$,
and the paramagnetic parts are in the opposite order,
$\sigma_{\text{iso}}^{\text{param}}(Lr,\ Rl)<\sigma_{\text{iso}}^{\text{param}}(Ll,\ Rr)$.
The resulting sign of the chiral shift is dominated by the paramagnetic terms,
$\sigma_{\text{iso}}(Ll,\ Rr)-\sigma_{\text{iso}}(Lr,\ Rl)=+0.036\,05$ ppm.

In Table I for case (a) we note that $\sigma_{\text{compressed}}^{\text{diam}}>\sigma_{\text{reference}}^{\text{diam}}$ since the electron is, on average, closer to the naked spin. $\sigma_{\text{stretched}}^{\text{diam}}<\sigma_{\text{reference}}^{\text{diam}}$ since the electron is, on average, farther from the naked spin. In Table II for case (b) we note that $\sigma_{\text{compressed}}^{\text{diam}}>\sigma_{\text{reference}}^{\text{diam}}$ since the electron is, on average, closer to the naked spin. This is more pronounced in case (b) than in case (a) since those parts of the helix that contribute the largest $1/\rho$ are essentially unchanged upon compression in (a), but are changed quite a lot upon compression in (b). $\sigma_{\text{stretched}}^{\text{diam}}<\sigma_{\text{reference}}^{\text{diam}}$ since the electron is, on average, farther from the naked spin. $[\sigma_{\text{compressed}}^{\text{diam}}-\sigma_{\text{reference}}^{\text{diam}}]>[\sigma_{\text{reference}}^{\text{diam}}-\sigma_{\text{stretched}}^{\text{diam}}]$ since compression gives larger $1/\rho$ for all points on the helix.

TABLE III. The diamagnetic part of the shielding tensor for the naked spin from the electron on a helix and from the electron on a circle of radius a; g stands for ground state.

	(i)		(ii)	
Term ρ	Electron on a helix [case (a)] ppm var	Electron on a circle, naked spin at the center ppm $\rho=a=3.260$ Å	Electron on a helix, [case (b)] ppm var	Electron on a circle naked spin below center ppm $\rho=[a^2+s^2]^{1/2}=3.8246$ Å
$\sigma_{XX}^{\text{diam}}=(e^2/2mc^2)\cdot\langle g\vert(y^2+z^2)/\rho^3\vert g\rangle$	2.213 75 (2.160 99)[a]	2.161	2.325 48	2.345 65
$\sigma_{YY}^{\text{diam}}=(e^2/2mc^2)\cdot\langle g\vert(x^2+z^2)/\rho^3\vert g\rangle$	2.191 44 (2.160 99)[a]	2.161	2.300 69	2.345 65
$\sigma_{ZZ}^{\text{diam}}=(e^2/2mc^2)\cdot\langle g\vert(x^2+y^2)/\rho^3\vert g\rangle$	4.042 84 (4.321 98)[a]	4.322	2.711 56	2.676 52
$\sigma_{\text{iso}}^{\text{diam}}=(e^2/3mc^2)\cdot\langle g\vert 1/\rho\vert g\rangle$	2.816 01 (2.881 32)[a]	2.881	2.445 91	2.455 94

[a]For $\beta=0$.

IV. DISCUSSION

Some interesting symmetry consequences for the components of the shielding tensor become transparent in this simple model for chiral systems and are worth noting (see Tables I and II).

(i) The matrix element $\langle 1\vert L_x\vert n\rangle$ is zero for even n for case (a), whereas it is nonzero for both odd and even n in case (b) because L_x is even; $\langle 1\vert L_y\vert n\rangle$ and $\langle 1\vert L_z\vert n\rangle$ are zero for n odd in case (a) whereas they are nonzero for both odd and even n in case (b) because L_y and L_z are odd relative to the origin.

(ii) In case (a) only odd n states contribute to $\sigma_{XX}^{\text{param}}$ and only even n states contribute to $\sigma_{YY}^{\text{param}}$ and $\sigma_{ZZ}^{\text{param}}$ whereas both odd and even n states contribute to these paramagnetic terms in case (b).

(iii) In case (a) $\sigma_{XY}^{\text{param}}$ and $\sigma_{YX}^{\text{param}}$ vanish for n even (due to $\langle 1\vert L_x\vert n\rangle$) and vanish for n odd (due to $\langle 1\vert L_y\vert n\rangle$); $\sigma_{XZ}^{\text{param}}$ and $\sigma_{ZX}^{\text{param}}$ vanish for n even (due to $\langle 1\vert L_x\vert n\rangle$) and vanish for n odd (due to $\langle 1\vert L_z\vert n\rangle$); $\sigma_{YZ}^{\text{param}}$ and $\sigma_{ZY}^{\text{param}}$ are nonzero only for even n states, they vanish for n odd (due to both $\langle 1\vert L_y\vert n\rangle$ and $\langle 1\vert L_z\vert n\rangle$).

(iv) Since the axis of the helix is along the Z axis and in case (a) the helix has $C_{2(x)}$ symmetry, the only off-diagonal tensor components are YZ and ZY. Both diamagnetic and paramagnetic terms contribute to these off-diagonal tensor components in the symmetric tensor. Only the paramagnetic term contributes to the antisymmetric tensor. In case (b) there is no such symmetry, so off-diagonal components are nonvanishing for both the symmetric and antisymmetric tensor of case (b).

(v) In case (b) $\sigma_{XY}^{\text{param}}$ and $\sigma_{YX}^{\text{param}}$ are much, much smaller than the others since $\langle 1\vert L_x\vert n\rangle$ and $\langle 1\vert L_y\vert n\rangle$ are smaller than $\langle 1\vert L_z\vert n\rangle$, term by term. Similarly $\sigma_{XY}^{\text{diam}}$ and $\sigma_{YX}^{\text{diam}}$ are much, much smaller than the others since z is positive at every point, and contributes to xz and yz products, whereas x and y coordinates are of both signs.

Some interesting comparisons can be made of the shielding of a naked spin by an electron on a helix against the shielding by an electron on a circle. For the diamagnetic shielding, the results for electron on a helix, naked spin at the center, case (a), should be close to the results for electron on a circle of radius a, naked spin at the center, $a=3.260$ Å, $\rho=\text{const}=a$. The diamagnetic shielding is easily calculated for the electron on a circle, naked spin at the center:

$$\sigma_{XX}^{\text{diam}}=(e^2/2mc^2)\cdot\langle 0\vert(y^2+z^2)/\rho^3\vert 0\rangle$$
$$=(e^2/2mc^2)\cdot(1/2a),$$

$$\sigma_{ZZ}^{\text{diam}}=(e^2/2mc^2)(1/a).$$

Furthermore, when $\beta\rightarrow 0$ and $k=1$, the results for the diamagnetic shielding of an electron on a helix, naked spin at the center, case (a), should reduce exactly to the results for the electron on a circle of radius a, naked spin at the center.

On the other hand, for the diamagnetic shielding, the results for electron on a helix, naked spin at the end, case (b), should be close to the results for electron on a circle of radius a, naked spin below center, located at $z=-s=-bk\pi$. For the electron on a halo, we use $s=bk\pi=2.0$ Å, $\rho=\text{const}=[a^2+s^2]^{1/2}=3.8246$ Å. The diamagnetic shielding for the electron on a circle, naked spin below center, is given by

$$\sigma_{XX}^{\text{diam}}=(e^2/2mc^2)\cdot\langle 0\vert(y^2+z^2)/\rho^3\vert 0\rangle$$
$$=(e^2/2mc^2)\cdot[1/\rho-a^2/2\rho^3],$$

$$\sigma_{ZZ}^{\text{diam}}=(e^2/2mc^2)(a^2/\rho^3).$$

In Table III we compare the magnitudes of the diamagnetic term for case (a) with that for an electron on a circle, located at the center of the case (a) helix. We find that the diamagnetic part of the shielding does indeed become equal to that of the electron on a circle as the limiting situation, when $\beta\rightarrow 0$ and $k=1$. Because of boundary conditions, the highest probability for the electron in the ground state of the helix case (b) is in the middle ($\sin^2\theta$), thus very similar to an electron on a halo above the naked spin. Indeed, Table III shows that the diamagnetic shieldings for case (b) is nearly identical to that of the electron halo.

An interesting point about whether the electron on a helix truly reduces to an electron on a circle in the limit $\beta\rightarrow 0$ and $k=1$ is considered here. There is one term in the paramagnetic shielding for an electron on a helix that does not vanish as $\beta\rightarrow 0$:

$$\langle 1\vert[-ia^2/(a^2+\beta^2)]\partial/\partial\theta\vert n\rangle$$
$$\cdot\langle n\vert[-ia^2/\rho^3(a^2+\beta^2)]\partial/\partial\theta\vert 1\rangle.$$

This does not vanish for n even in both case (a) and case (b). In fact, in both case (a) and case (b), this contribution to the paramagnetic shielding as $\beta \rightarrow 0$ reduces to the same expression:

$$\sigma_{ZZ}^{\text{param}} = -(e^2/2mc^2)(32/a\pi^2)\cdot\Sigma_{n=2}^{\text{even}}\{n^2/(n^2-1)^3\}.$$

Why does the paramagnetic shielding of a naked spin exposed to an electron on a helix with $\beta=0$ and $k=1$ not reduce to the same zero paramagnetic shielding as for the naked spin exposed to the electron on a circle? The electron on a helix cannot reduce to the electron on a circle for all properties because of the boundary conditions on the wave functions of the helix; the functions all have to vanish at the ends of the helix. The electron on a circle does not have the same boundary conditions. For a specific eigenstate, one could imagine cutting the circle at a node so that it looks like a one-turn helix with a vanishing pitch and then compare any properties calculated as expectation values for this eigenstate of the circle with those for a one-turn helix ($k=1$) with a vanishing pitch ($\beta \rightarrow 0$). However, matrix elements between different eigenstates cannot be compared unless the two states have one node at the same point, at which the cut can be made. Since paramagnetic shielding involves matrix elements between the ground and all other states, there is no possibility of cutting at the same point for all of them; thus the paramagnetic shielding for an electron on a helix cannot reduce to that for an electron on a circle.

We already noted that only the paramagnetic part of the shielding contributes to the antisymmetric shielding tensor. The relationship between the nonvanishing antisymmetric tensor for a system and chirality needs to be clarified here. As discussed in Paper I,[9] when the chiral point group is lower than D_n, T, or O, chirality is a sufficient condition for the existence of an antisymmetric contribution to the shielding tensor. It is not a necessary condition. The fact that $[\sigma_{YZ}-\sigma_{ZY}]_{Ll} \neq [\sigma_{YZ}-\sigma_{ZY}]_{Lr}$ is both necessary and sufficient that Ll and Lr are diastereomers. Hence, like the shifts themselves, the antisymmetric terms may be measures of chirality.

Going from the left- to the right-handed helix changes the sign of the antisymmetric part of the tensor, but the sign of the antisymmetric part is not intrinsic to the handedness. We establish this by comparing the shielding of a naked spin in the electron on a helix with that in the Ne_8 helix. For example, in Table IV, we compare the Ne_8 helix and the electron on a helix, both right-handed. The order of the diagonal tensor elements is $\sigma_{XX} > \sigma_{YY} > \sigma_{ZZ}$. The signs of the off-diagonal symmetric parts are positive for both systems, but the signs of the antisymmetric parts are opposite.

In Table V, the naked spin at the end of the Ne_8 helix can be compared with case (b). Because of the boundary conditions, the electron on a helix provides very small off-diagonal symmetric terms, and even smaller antisymmetric terms, but the number of nonvanishing components are as found for the Ne_8 helix. Only the $[\sigma_{YZ}+\sigma_{ZY}]$ components are dominated by paramagnetic terms.

Finally, we consider the sign of the chiral shift,

TABLE IV. Comparison of the shielding tensor at the origin of the same right handed helix, one with eight Ne atoms on it, the other with one electron on it.

Ne_8 helix Full tensor			Electron on a helix [case (a)]		
1.1267	0	0	2.106 25	0	0
0	0.6934	+0.9742	0	2.008 25	0.278 249
0	+0.9748	−1.8249	0	0.177 431	0.591 864
Symmetric tensor					
1.1267	0	0	2.106 25	0	0
0	0.6934	+0.9745	0	2.008 25	0.227 84
0	+0.9745	−1.8249	0	0.227 84	0.591 864
Antisymmetric tensor					
0	0	0	0	0	0
0	0	−0.0003	0	0	+0.050 409
0	+0.0003	0	0	−0.050 409	0

$$\sigma_{\text{iso}}(Ll) - \sigma_{\text{iso}}(Lr) = +0.036\,05 \text{ ppm} = \sigma_{\text{iso}}(Rr) - \sigma_{\text{iso}}(Rl).$$

Of this isotropic chiral-shift, −0.024 13 ppm comes from the diamagnetic part and +0.060 18 ppm comes from the paramagnetic part. The paramagnetic part dominates the chiral shift for the electron on a helix.

The parameters for the helix in this work were chosen to be the same as that used for the Ne_8 helix in Papers I and II[7,9] so that comparison may be made with these systems. We already mentioned in the Results section four observations about the components of the shielding tensors in the model system that are the same as those for naked spin or Xe atom in the Ne_8 helix. Now we consider the sign of the isotropic chemical shift between the diastereomers. The relative order of the isotropic shieldings of the naked spin in the diastereomeric electron on a helix systems are found to be

Lr, Rl are less shielded than LL, Rr in $n@e^-$helix,

the same order as we found for for r and l helices of negative charges,

Lr, Rl are less shielded than Ll, Rr in $n@Ne_8$.

On the other hand, we found for r and l helix of positive charges, the relative order was

Lr, Rl are more shielded than Ll, Rr in $n@Ne_8$

and $Xe@Ne_8$.

Figure 1 compares the electron on a helix model against the Ne_8 helix with the naked spin at the center of the helix in all cases, not really a fair comparison since perturbation, by a helix (radius=6.3706 Å) of partial charges $\pm 0.061\,953e$, on Ne_8 has moved the shielding of the naked spin by a large amount! On the other hand, the perturbation afforded by changing the pitch of the helix in the simple model is symmetrical about the unperturbed helix, of course. This plot definitely shows that it is not possible to determine, *a priori*, the sign of diastereomeric chiral shifts: (*Lr, Rl*) can be more or less shielded than (*Ll, Rr*).

TABLE V. Comparison of the shielding tensor at the end of a helix, one with eight Ne atoms on it, the other with one electron on it.

Ne_8 helix Full tensor			Electron on a helix [case (b)]		
0.784 5	0.201 5	−0.265 4	1.830 39	0.007 627 75	0.021 217 9
0.202 4	0.173 0	−0.038 4	0.007 627 54	1.788 75	−0.180 881
−0.266 6	−0.037 7	−0.961 0	0.021 219 7	−0.180 878	0.077 019 4
Symmetric tensor					
0.784 5	0.201 95	−0.266 0	1.830 39	0.007 627 64	0.021 218 8
0.201 95	0.173 0	−0.038 05	0.007 627 64	1.788 75	−0.180 879
−0.266 0	−0.038 05	−0.961 0	0.021 218 8	−0.180 879	0.077 019 4
Antisymmetric tensor					
0	−0.000 45	+0.000 6	0	1.076×10^{-7}	-9.15×10^{-7}
+0.000 45	0	−0.000 35	-1.076×10^{-7}	0	-1.36×10^{-6}
−0.000 6	+0.000 35	0	9.15×10^{-7}	1.36×10^{-6}	0

V. GRAND CONCLUSIONS

In our series of three papers we investigated the manifestation of chirality in a scalar measurement, namely the nuclear magnetic shielding tensor. As noted, chirality appears explicitly if and only if the given chiral system is coupled to another chiral system. If the two chiral systems are bound together, that is diastereomerism.

In Papers I and II,[7,9] our chiral systems were of neon atom helices. The additional bound chiral system was simulated by chiral potentials: positive or negative point charges arranged in helices. In Paper III (this work) an electron constrained to a helix served as our chiral system. Varying the pitch of the helix became our additional chiral potential, our diastereomers.

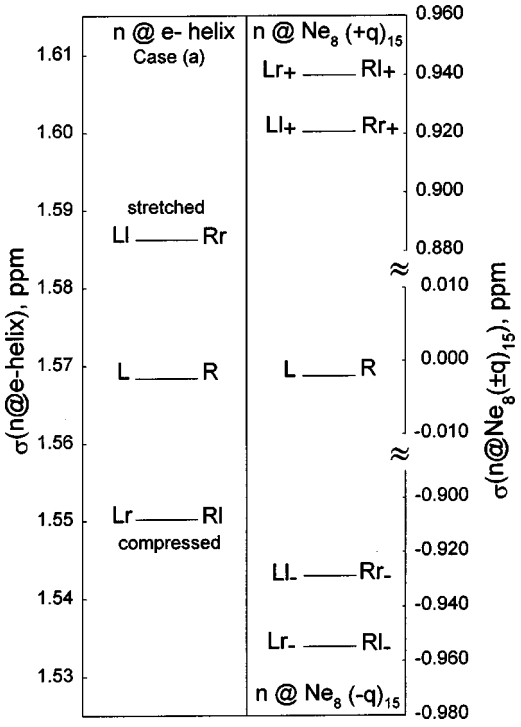

FIG. 1. Level diagram comparing shielding and energy of various chiral systems. The splitting between the shieldings of diastereomeric pairs is the chiral shift.

In Paper I we investigated the shielding tensor of a Xe atom placed in the helices. That is, we looked at induced chirality, or, for want of a better description, ''induced diastereomerism.'' In Paper II (and Paper III) we replaced the Xe by a naked spin. This allowed us to examine explicitly how the Xe electrons are affected by their interaction with diastereomers.

In Paper I we first calculated the complete shielding tensors of Xe imbedded in helices of 7-, 8-, and 15-Ne atoms without the added chiral potentials. The 7- and 15-Ne helices being of lower symmetry contributed more elements than the 8-Ne helix. These extra elements are boring so we focused all analysis on the Ne_8 helix. All three helices presented a stringent test of the pairwise addition model of tensors of one of us. We used the ''dimer tensor model'' to calculate the second rank (symmetric tensor) and scalar shift. The results compared favorably to the *ab initio* calculations. Hence the pairwise model should be useful for calculating the shielding tensors of oriented interacting van der Waals complexes. It provides no antisymmetric tensor elements. Of particular importance is the result that replacing tethers with given chiral potentials appears an adequate method of simulating diastereomerism. This result holds not only for Xe but for the naked spin as well.

By investigating both Xe and naked spins in the presence of the same Ne diastereomers we were able to clearly look at induced diastereomerism. In particular we looked at the (single) antisymmetric tensor element splitting. It is an order of magnitude larger in Xe than in the naked spin. We suggest that this is a new manifestation of diastereomerism.

In Paper III we calculated the nuclear magnetic shielding tensor of a naked spin interacting with an electron constrained to a helix. Here diastereomerism is mimicked by changing the pitch of the helix. The model has many virtues. First of all, all aspects of the Ne naked spin diastereomers may be reproduced with equivalent parameters (radius, pitch, number of turns). The simple model captures the essence of the more complicated models. Second, the shielding tensor obtained is exact. Hence the diamagnetic and paramagnetic terms may be exactly calculated. Although we chose the origin to be at the position of the spin, we could have calculated

the relative weights of the paramagnetic and diamagnetic contributions for any change of gauge origin. Tinoco and Woody's model has proved to be an extremely useful model of chirality.

As we said in the beginning of Paper I, our work was inspired by the experiments of the Pines group. We believe that we may be optimistic about calculating the splittings of the shielding tensor of Xe in chiral cages with chiral tethers. We also hope that our work may inspire experiments which would measure shieldings of Xe and naked spins (or almost naked spins, i.e., ^{3}He) in chirally derivatized Buckyballs.

APPENDIX A: COMPONENTS OF THE ANGULAR MOMENTUM

In this Appendix we write out the components of the angular momentum defined as

$$L_k=(1/2\hbar)(\mathbf{r}_i\times\mathbf{p}_j-\mathbf{p}_i\times\mathbf{r}_j)\varepsilon^{ijk}, \tag{A1}$$

$$L_x=[-ia\beta/(a^2+\beta^2)][(\sin\theta-\theta\cos\theta)d/d\theta+\theta\sin\theta/2], \tag{A2}$$

$$L_y=[ia\beta/(a^2+\beta^2)][(\cos\theta+\theta\sin\theta)d/d\theta+\theta\cos\theta/2]), \tag{A3}$$

$$L_z=-[ia^2/(a^2+\beta^2)]d/d\theta. \tag{A4}$$

APPENDIX B: HERMITIAN OPERATORS

In this Appendix we write out the Hermitian operators

$$L_k/\rho^3\rightarrow 1/2[(1/\rho^3)L_k+L_k(1/\rho^3)], \tag{B1}$$

$$L_x/\rho^3\rightarrow(1/\rho^3)L_x+i[3a\beta^3/2(a^2+\beta^2)](\sin\theta+\theta\cos\theta)/\rho^5, \tag{B2}$$

$$L_y/\rho^3\rightarrow(1/\rho^3)L_y-i[3a\beta^3/2(a^2+\beta^2)]\times(\cos\theta+\theta\sin\theta)\theta/\rho^5, \tag{B3}$$

$$L_z/\rho^3\rightarrow(1/\rho^3)L_z+i[3a^2\beta^2/2(a^2+\beta^3)]\theta/\rho^5. \tag{B4}$$

ACKNOWLEDGMENTS

This work has been supported by The National Science Foundation (Grant No. CHE99-79259). R.A.H wishes to acknowledge numerous helpful conversations with I. Tinoco. In addition, he wishes to thank Professor I. Tobias for greatly helping his understanding of the relation between three-dimensional (3D) helices and 1D helices, in particular, for supplying him (R.A.H.) with the approximate angular momentum operators in 3D helical coordinates.

[1] I. Tinoco, Jr. and R. W. Woody, J. Chem. Phys. **40**, 160 (1964).
[2] E. U. Condon, W. Alter, and H. Eyring, J. Chem. Phys. **5**, 753 (1937).
[3] I. Tinoco, Jr. and M. P. Freeman, J. Phys. Chem. **61**, 1196 (1957).
[4] N. L. Balazs, T. R. Brocki, and I. Tobias, Chem. Phys. **13**, 141 (1976).
[5] J. J. Maki and A. Persoons, J. Chem. Phys. **104**, 9340 (1996).
[6] V. Krstić and G. L. J. A. Rikken, Chem. Phys. Lett. **364**, 51 (2002).
[7] D. N. Sears, C. J. Jameson, and R. A. Harris, J. Chem. Phys. **119**, 2691 (2003), preceding paper.
[8] Wolfram Research, Inc. Mathematica version 4, Champaign, IL, 1999.
[9] D. N. Sears, C. J. Jameson, and R. A. Harris, J. Chem. Phys. **119**, 2685 (2003), this issue.